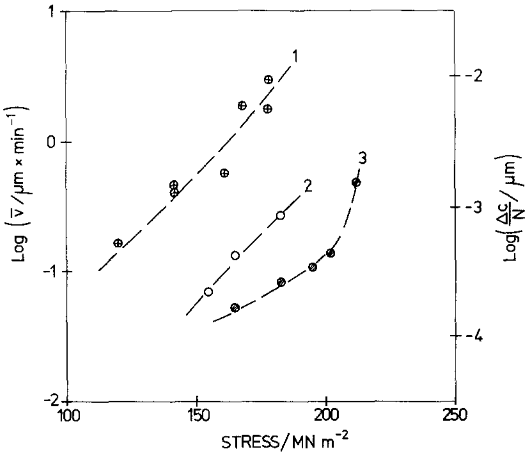

Figure 5 Peak stress, or constant stress, against logarithm of crack growth rate, and logarithm of crack velocity.

the experimental values $\sigma_0 = 195\,\text{MN}\,\text{m}^{-2}$ and $\sigma_0 = 218\,\text{MN}\,\text{m}^{-2}$ for the tensile strength of the "weak" and "strong" material respectively the initial flaw sizes $c_0 = 41\,\mu\text{m}$ and $c_0 = 33\,\mu\text{m}$ are obtained. These seem to be reasonable values, since they are nearly equal to the size of the largest grains.

The time to fracture, Δt, or the number of cycles to fracture, N, can be interpreted as the time, or cycles, taken for the cracks to grow from the initial size c_0 to the critical size, $c_0 + \Delta c$, under the applied stress conditions. The ratio $\Delta c/\Delta t$, or $\Delta c/N$, can be taken as a measure of the "gross average" crack velocity, or crack growth rate. Values of log $(\Delta c/\Delta t)$ and log $(\Delta c/N)$ have been calculated using the data of curves 1, 2 and 3 of Fig. 3 and plotted against maximum stress in Fig. 5. Since the crack velocity is usually related to the stress intensity factor K_I through a power function, such as $V = AK_I^n$, the "gross average" crack velocity is not a particularly meaningful parameter. It is used here only to show clearly and consistently how the crack velocity increases with stress and that for a given maximum stress value this velocity is in cyclic fatigue about 10 times greater than under static loading conditions.

It can therefore be concluded that the method of cyclic fatigue testing developed has been successfully applied to polycrystalline alumina and it has been shown that in this material cracks propagate faster under cyclic loads than under constant load conditions. This result suggests that alumina is susceptible to mechanical fatigue damage.

Acknowledgements

The author wishes to thank Mr A. Buckingham for his assistance with the machining of the specimens, the S.R.C. for financial support, and the C.R.F. of London University for an equipment grant.

References

1. D. A. KROHN and D. P. H. HASSELMAN, *J. Amer. Ceram. Soc.*, 55 (1972) 280.
2. C. P. CHEN and W. J. KNAPP, "Fracture Mechanics of Ceramics" (Plenum Press, 1973) p. 691.
3. B. K. SARKAR and T. G. T. GLINN, *Trans. Brit. Ceram. Soc.* 69 (1970) 199.
4. S. K. SINHA RAY, Ph.D. Thesis, University of London (1972).
5. A. G. EVANS and E. R. FULLER, *Metall. Trans.* 5 (1974) 27.
6. S. L. WILLIAMS, "Mechanical Properties of Engineering Ceramics", edited by W. Kriegel and H. Palmour (Interscience, 1961) p. 245.
7. R. W. DAVIDGE and G. TAPPIN, *Proc. Brit, Ceram. Soc.* 15 (1970) 47.
8. R. W. DAVIDGE and A. G. EVANS, *Mater. Sci. Eng.* 6 (1970) 281.
9. I. N. SNEDDON, *Proc. Roy. Soc.* A187 (1946) 229.

Received 9 August
and accepted 19 October 1977.

F. GUIU
Department of Materials,
Queen Mary College,
London, UK

Cathodoluminescence from slip planes in deformed MgO

Dislocations and their associated atmospheres of impurities or other point defects influence locally the luminescent properties of some ionic and semiconductor crystals as GaP [1] CdS [2] and GaAs [3, 4]. To investigate such influence the SEM in the cathodoluminescence mode has been frequently applied.

The effect of dislocations luminescence has been sometimes studied on plastically deformed crystals [5, 6] and the traces of slip planes in GaP [7] have been observed in the cathodoluminescence image. In the case of MgO crystals, it has been found [8, 9] that a concentrated load produced

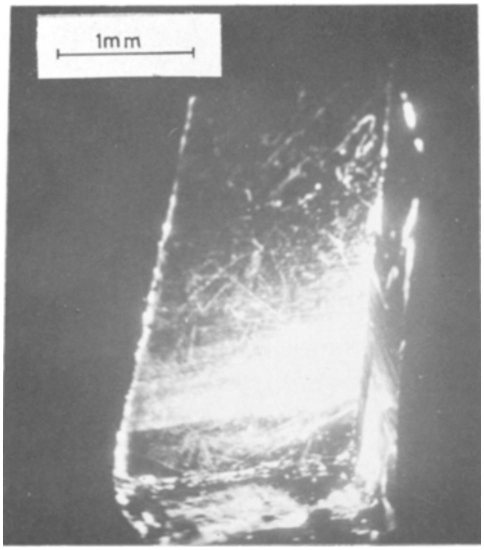

Figure 1 Cathodoluminescence image of a compressed MgO single crystal.

by indentation originates a cathodoluminescence rosette. Luminescence effects produced by plastic deformation have been also found in compressed MgO, CaO and SrO crystals illuminated by ultraviolet light [10].

The experiments described in [10] show that the increase of visible luminescence due to the compression is localized in the dislocation slip bands which can therefore be directly observed. However, due to the fact that the emission peak for deformed MgO occurs in the u.v. region, the visual intensity is rather low and therefore CaO and SrO are more useful for the photoluminescence studies of slip planes.

In the present work, the cathodoluminescence of compressed MgO single crystals was studied by means of SEM. The space distribution of light emission and in particular the slip planes were clearly observed.

The MgO single crystals used (W. C. Spicer and Co) had a purity of 99.9% and a size of 10 mm × 10 mm × 5 mm as received. The crystals were cleaved along (1 0 0) faces to their final dimensions of approximately 7 mm × 3 mm × 2 mm and compressed in a Hounsfield Tensometer type W. Some of the crystals were etched with a SO_4H_2 solution at 60° C to reveal the dislocation etch pits. Specimens were coated with a transparent conducting film and observed in the scanning electron microscope in the secondary and cathodoluminescence modes at 20 kV.

The cathodoluminescence image of a deformed crystal Fig. 1, shows an increased emission in those areas which have been subjected to high strains such as dislocation bands in compressed crystals, edges and surface scratches. It is always observed that the compression produces an increase in the crystal luminescence and that the emission is mainly localized at slip planes.

In Fig. 2 the secondary electron image and the

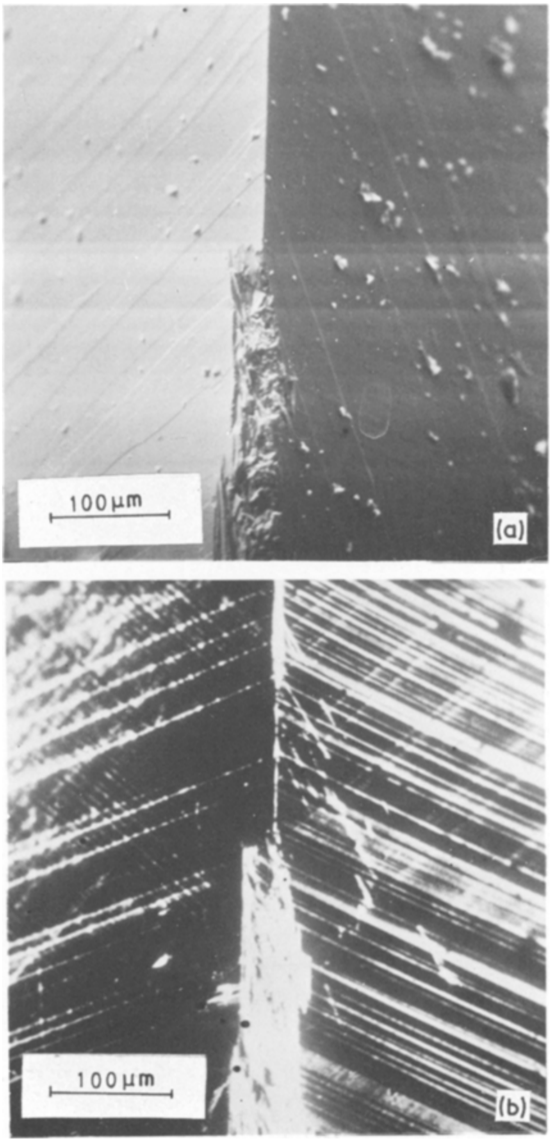

Figure 2 Area of the crystal shown in Fig. 1 observed at higher magnifications in (a) secondary electron mode, (b) cathodoluminescence mode.

cathodoluminescence image of the same area are shown. It can be seen that small irregularities in the surface do not influence the luminescence image of the slip planes. In compressed and subsequently etched crystals, it has been found that the areas with etch pits correspond to the areas with high luminescence which indicates that light emission is associated to the presence of the dislocations created during plastic deformation.

Some non-compressed specimens show lines of enhanced luminescence breaking into dots. The secondary electron image shows a correspondence between luminescence and dislocation etch pits (Fig. 3). The lines are located near the crystal edges and can be due to plastic deformation during cleavage. In other areas of the same crystals, where a high density of random distributed etch pits is present, no enhancement of cathodoluminescence was observed. From the above mentioned observations, it can be deduced that grown-in dislocations have a lesser influence on the cathodoluminescence than dislocations originated during plastic deformation. The difference between the two kinds of dislocations indicated that other defects, such as point defects and their clusters, which are formed with the dislocations during plastic deformation and remain close to them, can in fact determine the increase of cathodoluminescence with deformation.

In the case of MgO deformed by indentation [9] the cathodoluminescence was shown to be caused by interstitials, and the photoluminescence observations [10] of slip bands appeared to be associated with vacancy complexes, which agrees with the present observations. Some of the deformed crystals which showed slip planes in the cathodoluminescence image were annealed for 15 min at 800° C. The annealing caused a reduction in the slip planes luminescence. Due to the fact that an annealing at 800° C produces only minor changes in the dislocation arrangement in MgO [9, 11], while some of the smaller defects anneal out, the decrease of luminescence observed after such treatment indicates the influence of point defect complexed on the cathodoluminescence which appears with plastic deformation.

Acknowledgement

The help of Dr C. R. Serna throughout this work is gratefully acknowledged.

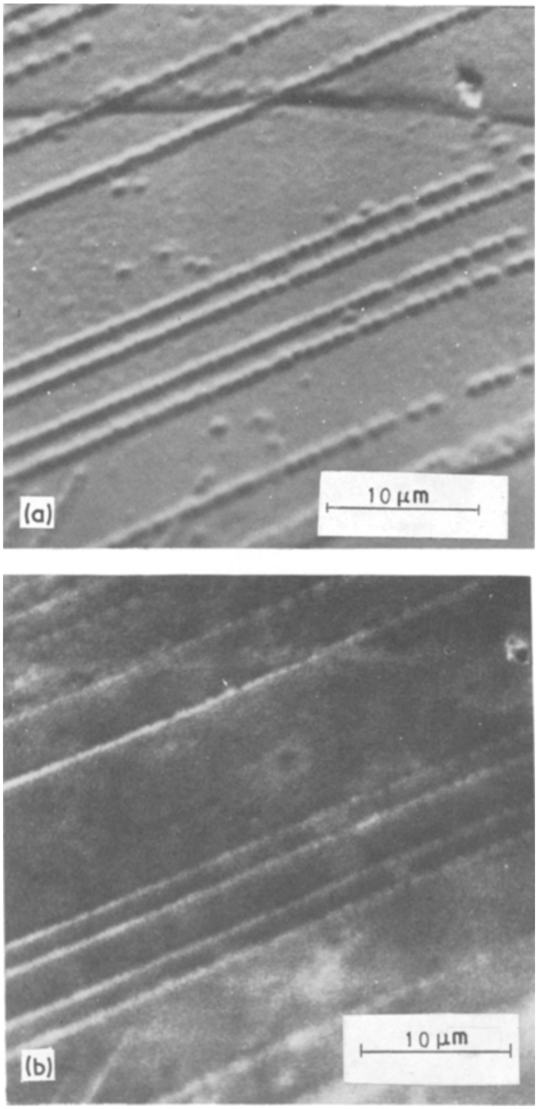

Figure 3 Area of an etched crystal observed in (a) secondary electron mode, (b) cathodoluminescence mode.

References

1. J. M. TITCHMARSH, G. R. BOOKER, W. HARDING and D. R. WIGHT, *J. Mater. Sci.* 12 (1977) 341.
2. O. BRUMMER and J. SCHREIBER, *Krist. u. Techn.* 9 (1974) 817.
3. L. J. BALK, E. KUBALEK and E. MENZEL, "IITRI/Scanning Electron Microscopy" edited by O. Johari (Chicago, 1976) p. 257.
4. D. A. SHAW and P. R. THORNTON, *J. Mater. Sci.* 3 (1968) 507.
5. B. TUCK and R. M. STURT, *ibid* 8 (1973) 295.
6. W. A. BRANTLEY, O. G. LORIMOR, P. D. DAPKUS, S. E. HASZKO and R. H. SAUL, *J. Appl. Phys.* 46 (1975) 2629.

7. S. M. DAVIDSON, M. Z. IQBAL and D. C. NORTHROP, *Phys. Stat. Sol. (a)* **29** (1975) 571.
8. V. N. ROZHANSKII and M. A. VELEDNITSKAYA, *Kristallografiya* **19** (1974) 1111.
9. M. A. VELEDNITSKAYA, V. N. ROZHANSKII, L. F. COMOLOVA, G. V. SAPARIN, J. SCHREIBER and O. BRUMMER, *Phys. Stat. Sol. (a)* **32** (1975) 123.
10. Y. CHEN, M. M. ABRAHAM, T. J. TURNER and C. M. NELSON, *Phil. Mag.* **32** (1975) 99.
11. R. J. STOKES, C. H. LI, *Discus. Faraday Soc.* **38** (1964) 233.

Received 9 August
and accepted 7 October 1977.

J. LLOPIS
J. PIQUERAS
L. BRU
Departamento de Fisica del Estado Solido,
Facultad de Ciencias Fisicas,
Universidad Complutense, Madrid

On the equilibrium transition temperature of thermoelastic martensitic transformations

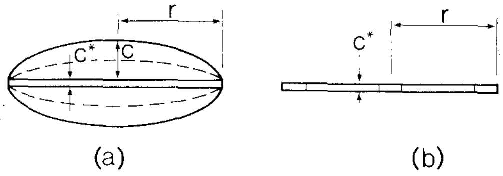

Figure 1 (a) Progressive thinning of an oblate spheroid of martensite with fixed radius during heating until a critical thickness C^* is attained. (b) Radial shrinkage of a plate of thickness C^*.

Recently, the thermodynamics of thermoelastic martensitic transformations have been studied by several investigators [1–6]. Although it is well known that the M_s[†] temperature should always lie below the T_0 temperature, there still exists an uncertainty in the location of the A_f temperature relative to T_0 [7–10]. An exact knowledge of the location of A_f relative to T_0 would be necessary if one attempts to determine approximately T_0 by bracketing it between M_s and A_f. Tong and Wayman [7, 8] and Olson and Cohen [9, 10] have analysed the thermodynamics of the process of formation of a single isolated martensite plate at M_s and its complete reversion to the HTP at A_f: However, different conclusions have been reached about the location of A_f relative to T_0. Tong and Wayman have assumed that the contribution of elestic strain energy to the total free energy difference between M and HTP is negligible at M_s and considered the internal frictional forces to be substantial. This necessarily led to the conclusion that $A_f > T_0$. They then proposed that T_0 can be approximated by:

$$T_0 = \tfrac{1}{2}[M_s + A_f].$$

However, the assumption of negligible elastic strain energy at M_s cannot be justified in view of the expected comparatively small chemical free energy difference.

In contrast, Olson and Cohen took into consideration the elastic strain energy and concluded that A_f could lie below T_0; therefore, the bracketing procedure proposed by Tong and Wayman cannot be generalized. They considered the case of an oblate spheroid of martensite having radius r and semithickness C, where $C \ll r$. (See Fig. 1). The total free energy difference (ΔG) accompanying formation of such martensite (in the absence of internal friction) can be written [11] as:

$$\Delta G(T)\,(\text{HTP}\rightarrow\text{M}) = \tfrac{4}{3}\pi r^2 C\Delta g_{\text{ch}}\,(\text{HTP}\rightarrow\text{M}) + \tfrac{4}{3}\pi r C^2 A + 2\pi r^2\sigma \qquad (1)$$

where A is an elestic strain energy constant such that (AC/r) is an elastic strain energy per unit volume and σ is an interfacial energy per unit area. The conclusion that $A_f < T_0$ was derived from the condition $\partial\Delta G/\partial r = 0$ and $\partial\Delta G/\partial c = 0$. That is, the martensite becomes completely unstable when the net forces (chemical and non-chemical) acting upon it vanish [9, 10].

However, this condition is expected to be satisfied at any temperature where thermoelastic equilibrium between M and HTP can be estab-

---

[†] M = martensite; HTP = high temperature phase; M_s = temperature at which transformation to M starts during cooling; T_0 = temperature at which $\Delta g_{\text{ch}}(\text{M}\rightarrow\text{HTP}, \text{HTP}\rightarrow\text{M}) = 0$, where Δg_{ch} is the chemical free energy difference per unit volume; A_f = temperature at which reversion of M to HTP is completed during heating.